Contribution from the Instituto de Quimica, Universidade de Sao Paulo, CP 20780, Sao Paulo, SP, Brazil, and Department of Chemistry, York University, North York, Ontario, Canada M3J 1P3

Spectroscopic and Kinetic Studies on a Series of Di- to Heptanuclear Tris(bipyrazine)ruthenium(II)-Pentacyanoferrate(II) Complexes in Aqueous Solution

H. E. Toma*[1a] and A. B. P. Lever*[1b]

Received March 19, 1985

The tris(bipyrazine)ruthenium(II) complex reacts with the aquapentacyanoferrate(II) ion, leading to a series of di- to heptanuclear pyrazine-bridged complexes, which were characterized by visible-UV and ^{1}H NMR spectroscopy and electrochemistry. Stopped-flow kinetics of the formation reactions were consistent with a stepwise mechanism, where the specific rates for the 1:1 to 1:6 complexes span the range 3.5×10^4–0.30 M^{-1} s^{-1}, following very closely the electrostatic formalisms applied to bimolecular reactions. The dissociation of the polynuclear complexes proceeds by a multistep consecutive mechanism, which was completely solved for the kinetic constants of the 1:1 to 1:6 species, and observed to lie in the range 4.6×10^{-4}–1.3×10^{-3} s^{-1}, respectively. The electronic spectra contain charge-transfer bands from iron(II) and from ruthenium(II) to bipyrazine.

Introduction

The tris(bipyrazine)ruthenium(II) complex[2-5] has recently been reported in the literature as a promising photocatalyst, having many complementary properties with respect to the tris(bipyridine)ruthenium(II) cation.[6,7] An interesting feature of the bipyrazine complex is the existence of six peripheral uncoordinated nitrogen atoms potentially available for protonation[4] or for coupling substrates in energy-transfer or electron-transfer processes. Coordination of transition-metal ions is also expected, particularly in the case of the π-back-bonding complexes such as the pentacyanoferrates.[8,9]

In this work we have explored the symmetric distribution of the peripheral nitrogen atoms in the tris(bipyrazine)ruthenium(II) complex to build up a series of di- to heptanuclear complexes with the pentacyanoferrate(II) ion, as illustrated in structure 1. The

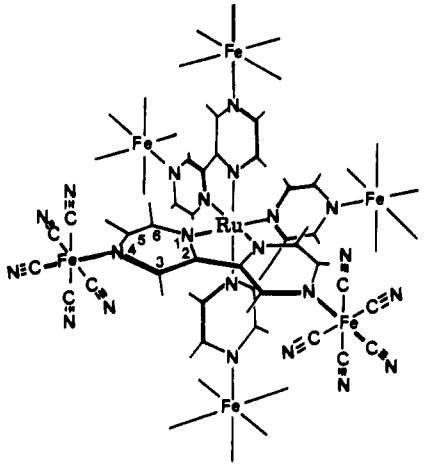

1

characterization of these new polynuclear complexes, based on visible-UV spectroscopy, electrochemistry, and the kinetics of the corresponding formation and dissociation reactions, is dealt with in this paper.

Experimental Section

$[Ru(bpz)_3](PF_6)_2$ and $Na_3[Fe(CN)_5NH_3]\cdot 3H_2O$ were prepared by literature methods.[3,10] The several successive polynuclear complexes $[Ru(bpz)_3(Fe(CN)_5)_n]^{(2-3n)+}$ were obtained by reacting the bipyrazine complex, previously dissolved in aqueous solution, with the amminepentacyanoferrate(II) salt, under an argon atmosphere. The ammonia released in the process was neutralized with hydrochloric acid.

The $[(bpz)_2Ru(bpz)Fe(CN)_5]^-$ complex was isolated as a dark green solid by precipitating with ethanol, after converting the $[Ru(bpz)_3](PF_6)_2$ salt into the more soluble chloride form, with tetraphenylarsonium chloride (Aldrich). Analysis of the binuclear product kept under vacuum for 3 days, in the presence of calcium chloride, was consistent with the composition $NaRuFeC_{29}N_{17}H_{18}\cdot 8H_2O$. Anal. Calcd: C, 37.53; N, 25.65; H, 3.66. Found: C, 37.1; N, 25.6; H, 3.3.

Infrared spectra of the binuclear complex dispersed in Nujol (or in KBr pellets) were recorded on a Beckman IR-33 instrument. The presence of the pentacyanoferrate(II) group was detected by the characteristic absorption bands at 2080 (w) and 2050 (s) cm^{-1}. The vibrational frequencies of the bipyrazyl ligand were observed at 1590 (s), 1465 (m), 1415 (s), 1315 (m), 1275 (m), 1180 (m), 1165 (s), 1105 (w), 1075 (m), 1050 (w), 1025 (m), 838 (m), and 655 (m) cm^{-1}. Strong absorption bands at 3350 and 1640 cm^{-1} observed with the Nujol mulls confirm the presence of a large amount of water in the solid (s = strong, m = medium, w = weak).

The electronic spectra of the complexes in the visible-UV region were recorded on a Cary 17 or on a diode-array Hewlett-Packard 8451 spectrophotometer, fitted with thermostated cell compartments. The spectra obtained by dissolving the binuclear solid in aqueous solution were identical with those recorded for the species generated directly in solution: λ_{max} = 692, (log ϵ = 3.92), 500 (shoulder, sh), 442 (4.18), 415 (sh), 343 (sh), 302 (4.65), 268 (sh), 238 nm (4.47). The electronic spectra of the solid dispersed in PVA film were similar to those of the aqueous solutions, except for an enhancement of the shoulder at 343 nm and a bathochromic shift of the absorption bands at 442 and 692 nm to 460 and 768 nm, respectively.

Nuclear magnetic resonance spectra were recorded on a Varian T-60 spectrometer, at a probe temperature of 33 °C. The measurements were made in D_2O, with use of a 0.03 M solution, prepared under argon atmosphere.

The kinetics of formation of the polynuclear complexes were investigated with a Durrum D-110 stopped-flow apparatus, equipped with a Kel-F flow system. The aquapentacyanoferrate(II) ion employed for the kinetics was generated by the aquation of the amminepentacyanoferrate(II) complex (10^{-4} M), under an argon atmosphere. Formation of the 1:1, 1:2, and 1:3 species was studied independently, starting from the preceding mononuclear, 1:1, and 1:2 complexes, respectively, in excess (10^{-4}–10^{-5} M), and reacting with the aquapentacyanoferrate(II) complex (10^{-5}–10^{-6} M). The kinetics were monitored at 700, 600, and 500 nm, respectively. The formation of the 1:4, 1:5, and 1:6 species requires a high concentration of the aquapentacyanoferrate(II) complex to be complete. In this case, the kinetics were investigated by starting from the 1:3 complex (10^{-5} M) and reacting with a large excess of $[Fe(CN)_5H_2O]^{3-}$ (10^{-2}–10^{-3} M). The concentrations of the aquapentacyanoferrate(II) complex were corrected for the dimerization reaction,[11] which leads to the less reactive $[Fe_2(CN)_{10}]^{6-}$ species, with K = 80 M.

The kinetics of dissociation of the polynuclear complexes were studied in the presence of a large excess of dimethyl sulfoxide (Me_2SO), with a Cary 14 spectrophotometer. The Me_2SO ligand was chosen for this study

(1) (a) Universidade di Sao Paulo. (b) York University.
(2) Crutchley, R. J.; Lever, A. B. P. *J. Am. Chem. Soc.* **1980**, *102*, 7128.
(3) Crutchley, R. J.; Lever, A. B. P. *Inorg. Chem.* **1982**, *21*, 2276.
(4) Crutchley, R. J.; Kress, N.; Lever, A. B. P. *J. Am. Chem. Soc.* **1983**, *105*, 1170.
(5) Rillema, D. P.; Allen, G.; Meyer, T. J.; Conrad, D. *Inorg. Chem.* **1983**, *22*, 1617.
(6) Kalyanasundaram, K. *Coord. Chem. Rev.* **1979**, *46*, 159.
(7) Sutin, N.; Creutz, C. *Pure Appl. Chem.* **1980**, *52*, 2717.
(8) (a) Toma, H. E.; Malin, J. M. *Inorg. Chem.* **1973**, *12*, 1039. (b) Toma, H. E.; Batista, A. A.; Gray, H. B. *J. Am. Chem. Soc.* **1982**, *104*, 7509.
(9) Yeh, A.; Haim, A. *J. Am. Chem. Soc.* **1985**, *107*, 369.
(10) Brauer, G. "Handbook of Preparative Inorganic Chemistry", 2nd ed.; Academic Press: New York, 1965; Vol. 2, p 1511.
(11) Emschwiller, G. *C. R. Hebd. Seances Acad. Sci.* **1964**, *259*, 4281.

0020-1669/86/1325-0176$01.50/0

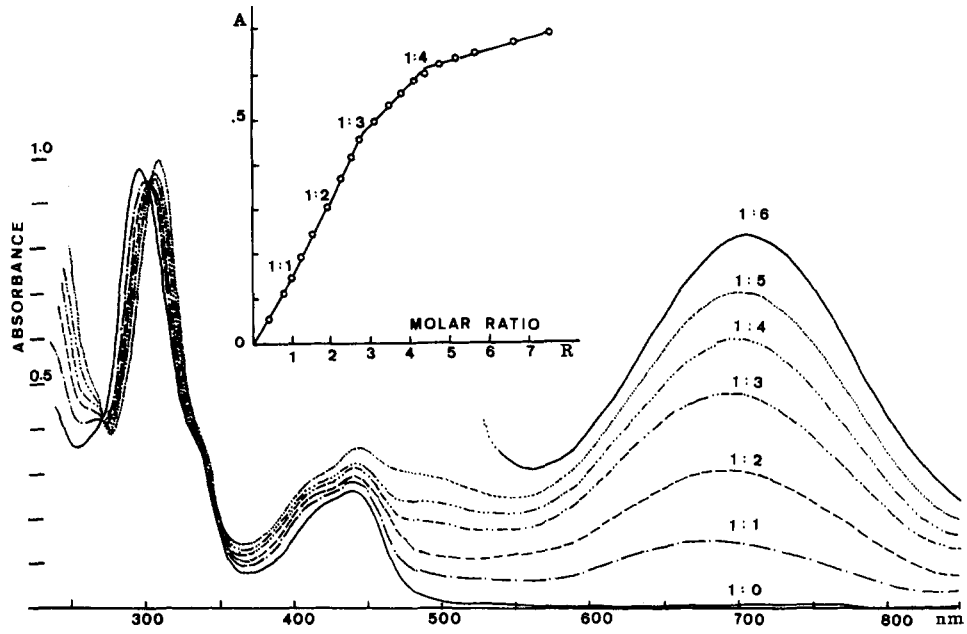

Figure 1. Absorption spectra of the $Ru(bpz)_3^{2+}$ complex (1.8×10^{-4} M) and of the several polynuclear complexes containing $Fe(CN)_5^{3-}$, in aqueous solution and (inset) the titration plot at 700 nm (0.10 M acetate buffer, optical pathlength 0.100 cm, argon atmosphere).

because it forms with the aquapentacyanoferrate(II) ion a very stable complex that does not absorb in the visible and near-UV region.[12] In this way, the dissociation kinetics can be monitored directly by following the decay of the absorption band at 700 nm. The multistep consecutive kinetics were analyzed with a Microdigital TK-85 computer.

Cyclic voltammetry was carried out with Princeton Applied Research instrumentation, consisting of a Model 173 potentiostat and a Model 175 universal programmer. A glassy-carbon-disk electrode was employed for the measurements, with use of a conventional Luggin capillary arrangement with a Ag/AgCl (1 M KCl) reference electrode. A platinum wire was used as the auxiliary electrode. The measured potentials were converted to the NHE scale by adding 0.222 V.

Results and Discussion

The tris(bipyrazine)ruthenium(II) cation reacts with the aquapentacyanoferrate(II) complex, producing a series of deep green polynuclear complexes in aqueous solution. The 1:1 complex was isolated and analyzed; higher complexes were not isolated but were fully characterized by their visible–UV and NMR spectroscopy (see below). Typical visible–UV spectra of the complexes can be seen in Figure 1. The coordination of the $[Fe(CN)_5]^{3-}$ ion to the bipyridine complex leads to a new absorption band around 700 nm, similar to those previously reported for the related complexes[8,13,14] **2–4**.

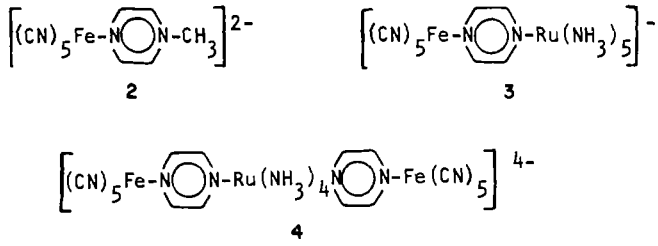

By analogy with these complexes, we assigned the absorption band at 700 nm to a $Fe(d_\pi) \rightarrow bpz(\pi^*(1))$ charge-transfer transition and the band near 445 nm to the characteristic $Ru(d_\pi) \rightarrow bpz(\pi^*(1))$ transition. An internal $\pi \rightarrow \pi^*$ transition in the bipyrazine ligand is observed around 300 nm. We defer discussion of these data until later in this paper.

Spectrophotometric titrations (Figure 1) with the aquapentacyanoferrate(II) ion, carried out in dilute solutions of the $[Ru(bpz)_3]^{2+}$ complex (1.8×10^{-4} M) are consistent with a stepwise, quantitative formation of the 1:1, 1:2, and 1:3 complexes. The corresponding molar absorptivities at the 700-nm band are 8.4×10^3, 16.9×10^3, and 2.6×10^4 M^{-1} cm^{-1}, respectively. Two inflections are observed in passing from the 1:3 to the 1:4 ($\epsilon = 3.4 \times 10^3$ M^{-1} cm^{-1}) and 1:5 species. Formation of the 1:5 complex requires a high molar ratio to overcome the dissociation equilibrium. The 1:6 complex can only be generated in concentrated solutions (e.g. 10^{-2} M) or in the presence of a very large excess of the aquapentacyanoferrate(II) ion. The molar absorptivities of the 1:5 and 1:6 complexes were estimated as 4.0×10^4 and 4.6×10^4 M^{-1} cm^{-1}, respectively.

NMR Spectra. The characterization of the several polynuclear complexes was carried out by recording the ^1H NMR spectra of the species generated from $[Ru(bpz)_3]Cl_2$ and $Na_3[Fe(CN)_5NH_3]\cdot 3H_2O$ at the appropriate molar ratios. Some typical results are shown in Figure 2. The ^1H NMR spectrum of the $[Ru(bpz)_3]^{2+}$ complex is consistent with an ABX system. The resonance signals observed at 10.05, 8.85, and 8.17 ppm are very similar to those previously in the literature[3] and were assigned to the H3, H5, and H6 protons, respectively. The chemical shifts for bipyrazine complexes[3,15] and related systems[16] have been discussed in terms of van der Waals deshielding, the inductive effect of ruthenium(II), and the diamagnetic anisotropy effect of the aromatic ring.

Coordination of the pentacyanoferrate(II) ion to the bipyrazine ligand produces dramatic changes in the NMR spectra, splitting the H3 peak and shifting the H5 and H6 peaks downfield and upfield, respectively. Previous studies[17,18] on the NMR spectra of the pentacyanoferrate(II) complexes of N-heterocyclic ligands have shown that the $[Fe(CN)_5]^{3-}$ moiety produces downfield shifts at the neighboring protons, due to the magnetic anisotropy associated with the cyanide ligands. The remote aromatic protons are shifted upfield. The observed downfield shifts for the adjacent H5 atoms and the upfield shifts for the remote H6 protons are in accord with the literature.

The $[Fe(CN)_5]^{3-}$ moiety has little influence on the remote H′5 and H′6 atoms, located in the vicinal aromatic ring of the bipyrazine ligand. Therefore, only a double pair of resonance peaks associated with the H5 and H6 atoms in the $[Fe(CN)_5]$-coor-

(12) Toma, H. E.; Malin, J. M.; Giesbrecht, E. *Inorg. Chem.* **1973**, *12*, 2084.
(13) Toma, H. E.; Santos, P. S. *Can. J. Chem.* **1977**, *55*, 3549.
(14) Toma, H. E. *J. Coord. Chem.* **1978**, *7*, 231.
(15) Dodsworth, E. S.; Lever, A. B. P.; Eryavec, G.; Crutchley, R. J. *Inorg. Chem.* **1985**, *24*, 1906.
(16) Lytle, F. E.; Petrosky, L. M.; Carlson, L. R. *Anal. Chim. Acta* **1971**, *57*, 239. Bryant, G. M.; Fergusson, J. E. *Aust. J. Chem.* **1971**, *24*, 441.
(17) Toma, H. E.; Malin, J. M.; Schmidt, C. F. *Inorg. Chem.* **1975**, *14*, 2924.
(18) Toma, H. E.; Malin, J. M. *Inorg. Chem.* **1973**, *12*, 2080.

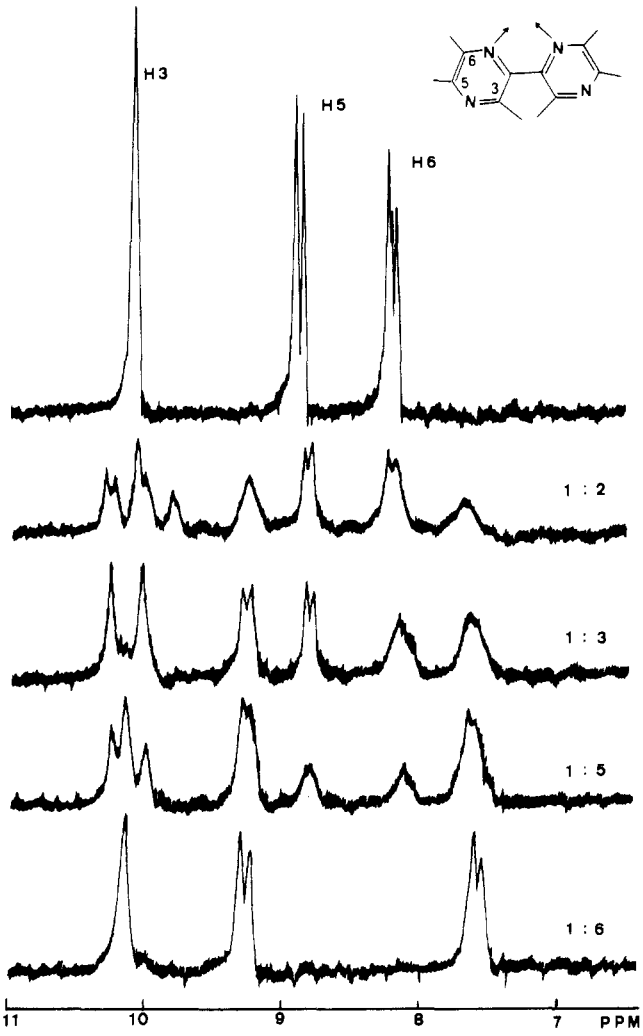

Figure 2. ^1H NMR spectra of the $Ru(bpz)_3^{2+}$ complex (0.03 M) and of the several polynuclear species containing $Fe(CN)_5^{3-}$, in D_2O (chemical shifts vs. Me_4Si).

dinated and uncoordinated pyrazine ring is observed, independently of the symmetry of the polynuclear complexes.

The H3 and H'3 atoms, however, are very close to the $[Fe(CN)_5]^{3-}$ moiety, being susceptible to the magnetic anisotropy to a different extent. Consequently, the H3 resonance signals split as a function of the symmetry of the polynuclear complexes. In the case of the 1:1 and 1:2 complexes, three sets of peaks are observed at 10.20, 10.05, and 9.75 ppm (Figure 2), corresponding to nonequivalent H3 and H'3 atoms in the $Fe(CN)_5$-coordinated and uncoordinated pyrazine rings. Only a pair of H3 and H'3 peaks is observed at 10.22 and 9.98 ppm for the 1:3 complex. This is consistent with a higher symmetry, where only one $[Fe(CN)_5]^{3-}$ ion is attached to each bipyrazine ligand. On the other hand, the doubly coordinated bipyrazine ligand can be detected in the spectra of the 1:4 and 1:5 complexes, by the new H3 peak appearing at 10.12 ppm. This peak grows in intensity for the highly symmetric 1:6 complex. Here, the original pattern, consisting of a single H3 peak, and two H5 and H6 doublets is observed again. The NMR spectra provide evidence for direct binding of the $[Fe(CN)_5]^{3-}$ groups to the bipyrazine nitrogen atoms and argue against the formation of simple ion multiplets.

Kinetic Studies. The formation of the polynuclear complexes involves substitution of water in the aquapentacyanoferrate(II) ion. The rates of substitution in this ion are practically independent of the nature of the neutral, attacking ligands,[18] being however sensitive to the charges of the anionic and cationic ligands.[9,13,14]

Because of the charge effects, the formation of the polynuclear complexes proceeds according to a successive, stepwise process.

The kinetics of reactions 1–3 were studied independently, starting from the mononuclear, 1:1, and 1:2 complexes, in excess, and reacting with the aquapentacyanoferrate(II) complex, in the stopped-flow apparatus. Typical first-order kinetics were observed

Table I. Kinetic and Equilibrium Data for Pyrazine-Bridged Ruthenium(II)–Cyanoiron(II) Polynuclear Complexes[a]

complex	k_f, M^{-1} s^{-1}	k_d, s^{-1}	K, M^{-1}	ref
$[Ru(bpz)_3Fe(CN)_5]^-$	3.5×10^4	4.6×10^{-4}	7.6×10^7	*b*
$[Ru(bpz)_3(Fe(CN)_5)_2]^{4-}$	1.2×10^4	8.5×10^{-4}	1.4×10^7	*b*
$[Ru(bpz)_3(Fe(CN)_5)_3]^{7-}$	1.2×10^3	1.1×10^{-3}	1.1×10^6	*b*
$[Ru(bpz)_3(Fe(CN)_5)_4]^{10-}$	8.0×10	1.2×10^{-3}	6.7×10^4	*b*
$[Ru(bpz)_3(Fe(CN)_5)_5]^{13-}$	1.0×10	1.25×10^{-3}	8.0×10^3	*b*
$[Ru(bpz)_3(Fe(CN)_5)_6]^{16-}$	0.30	1.3×10^{-3}	2.3×10^2	*b*
$[Ru(NH_3)_4pzFe(CN)_5]^-$	3.1×10^3	6.9×10^{-4}	4.5×10^6	13
$[Ru(NH_3)_4(pz)_2Fe(CN)_5]^-$	6.8×10^3	5.6×10^{-4}	1.2×10^7	14
$[Ru(NH_3)_4(pzFe(CN)_5)_2]^{4-}$	1.7×10^3	1.3×10^{-4}	1.3×10^6	14

[a] Conditions: 25 °C, ionic strength 0.100 M. [b] This work.

$$[Ru(bpz)_3]^{2+} + [Fe(CN)_5H_2O]^{3-} \underset{k_{10}}{\overset{k_{01}}{\rightleftharpoons}} [Ru(bpz)_3(Fe(CN)_5)]^- \quad (1)$$

$$[Ru(bpz)_3(Fe(CN)_5)]^- + [Fe(CN)_5H_2O]^{3-} \underset{k_{21}}{\overset{k_{12}}{\rightleftharpoons}} [Ru(bpz)_3(Fe(CN)_5)_2]^{4-} \quad (2)$$

$$[Ru(bpz)_3(Fe(CN)_5)_2]^{4-} + [Fe(CN)_5H_2O]^{3-} \underset{k_{32}}{\overset{k_{23}}{\rightleftharpoons}} [Ru(bpz)_3(Fe(CN)_5)_3]^{7-} \quad (3)$$

$$[Ru(bpz)_3(Fe(CN)_5)_3]^{7-} + [Fe(CN)_5H_2O]^{3-} \underset{k_{43}}{\overset{k_{34}}{\rightleftharpoons}} [Ru(bpz)_3(Fe(CN)_5)_4]^{10-} \quad (4)$$

$$[Ru(bpz)_3(Fe(CN)_5)_4]^{10-} + [Fe(CN)_5H_2O]^{3-} \underset{k_{54}}{\overset{k_{45}}{\rightleftharpoons}} [Ru(bpz)_3(Fe(CN)_5)_5]^{13-} \quad (5)$$

$$[Ru(bpz)_3(Fe(CN)_5)_5]^{13-} + [Fe(CN)_5H_2O]^{3-} \underset{k_{65}}{\overset{k_{56}}{\rightleftharpoons}} [Ru(bpz)_3(Fe(CN)_5)_6]^{16-} \quad (6)$$

for at least 2 half-lives. The second-order rate constants are shown in Table I. For the reactions 4 and 5, the kinetics were investigated by starting from the 1:3 complex and reacting with a large excess of $[Fe(CN)_5H_2O]^{3-}$. In this case, the kinetics were typically biphasic, corresponding to the stepwise formation of the 1:4 and 1:5 complexes. The kinetic constants k_{34} and k_{45} were calculated as 80 and 10 M^{-1} s^{-1}, from decomposition of the logarithmic plots, as described in the literature.[19] Formation of the 1:6 complex proceeds very slowly and was monitored with a Cary 14 instrument. The statistical errors are estimated to be less than 10% for the first three rate constants and 10–20% for the second three (Table I).

After correction for the statistical factor associated with the number of binding sites, the specific rates fall in a linear correlation with the charge product, Z_AZ_B, with an observed slope of 0.246, as shown in Figure 3. This kind of correlation can be fitted by equation 7 (calculated slope 0.215), where $\kappa = 0.329\mu^{1/2}$ (Å^{-1}),

$$\ln k_{cor} = \ln k_\infty - \frac{3.576}{r_A + r_B}\left[\frac{e^{-\kappa r_A}}{1 + \kappa r_B} + \frac{e^{-\kappa r_B}}{1 + \kappa r_A}\right]Z_AZ_B \quad (7)$$

with use of the estimated radii $r_A = 4.5$ Å and $r_B = 7.0$ Å for the cyanoiron and tris(bipyrazine)ruthenium(II) complexes, respectively. Equation 7 accounts quantitatively for the electrostatic effects involved in the approximation of ionic species in the activated collision complexes.[20] An exception is the formation of

(19) Espenson, J. H. "Chemical Kinetics and Reaction Mechanisms"; McGraw-Hill: New York, 1981; p 69.

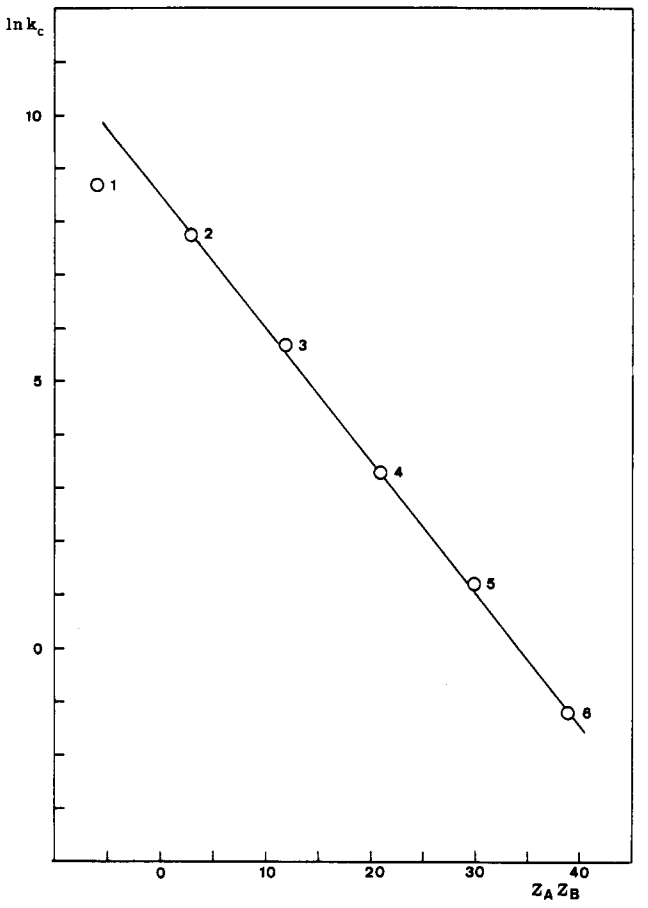

Figure 3. Plot of the logarithms of the kinetic constants for the formation of the binuclear (1) to heptanuclear (6) complexes, corrected for the number of binding sites, vs. the charge product Z_AZ_B of the reacting species (25 °C, ionic strength 0.100 M (NaCl), pH 4.5).

the 1:1 complex, as shown in Figure 3. In this case, the reaction involves two oppositely charged ions that can associate to form a stable precursor complex.[21]

The dissociation kinetics for the polynuclear complexes were investigated in the presence of a large excess of Me_2SO. For the 1:1 complex, the kinetics follow a first-order rate law for at least 3 half-lives. Saturation behavior was observed at Me_2SO concentrations above 10^{-2} M, consistent with the scheme

$$[Ru(bpz)_3Fe(CN)_5]^- + H_2O \underset{k_{01}}{\overset{k_{10}}{\rightleftharpoons}} [Ru(bpz)_3]^{2+} + [Fe(CN)_5H_2O]^{3-}$$

$$[Fe(CN)_5H_2O]^{3-} + Me_2SO \underset{k_{-Me_2SO}}{\overset{k_{Me_2SO}}{\rightleftharpoons}} [Fe(CN)_5Me_2SO]^{3-} + H_2O \quad (8)$$

where k_{10} is equal to 4.6×10^{-4} s^{-1}, and k_{01}, k_{Me_2SO}, and k_{-Me_2SO} have already been measured as 3.5×10^4 M^{-1} s^{-1}, 370 M^{-1} s^{-1}, and 7.5×10^{-5} s^{-1}, respectively.[8]

The dissociation of the 1:2 to 1:6 polynuclear complexes proceed according to a consecutive mechanism and were investigated at the saturation point. In this way, the kinetics can be described by a consecutive irreversible scheme, such as

$$A_1 \xrightarrow{k_1} A_2 \xrightarrow{k_2} A_3 \ldots A_{n-1} \xrightarrow{k_{n-1}} A_n \quad (9)$$

The set of differential equations for this mechanism has already been solved, in terms of the general expression (10), which describes the concentration of the intermediates existing at any time during the reaction:[22]

$$[A_{n-1}] = (p_{n-1})_1 e^{-k_1 t} + (p_{n-1})_2 e^{-k_2 t} + \ldots + (p_{n-1})_{n-1} e^{-k_{n-1} t} \quad (10)$$

where

$$(p_{n-1})_1 = \frac{k_1 k_2 k_3 \ldots k_{n-2}[A_1]_0}{(k_2 - k_1)(k_3 - k_1)\ldots(k_{n-1} - k_1)}$$

$$(p_{n-2})_2 = \frac{k_1 k_2 k_3 \ldots k_{n-2}[A_1]_0}{(k_1 - k_2)(k_3 - k_2)\ldots(k_{n-1} - k_2)}$$

$$(p_{n-1})_{n-1} = \frac{k_1 k_2 k_3 \ldots k_{n-2}[A_1]_0}{(k_1 - K_{n-1})(k_2 - k_{n-1})\ldots(k_{n-2} - k_{n-1})}$$

On the other hand, the absorbance measured at 700 nm can be expressed by

$$A_t = \epsilon_1[A_1] + \epsilon_2[A_2] + \ldots + \epsilon_n[A_n] \quad (11)$$

Starting from the 1:2 complex, the k_{21} dissociation constant was calculated as 8.5×10^{-4} s^{-1}, by substituting k_{10} and ϵ_i into eq 10 and 11 and carrying out a computational analysis to fit accurately the kinetic plots shown in Figure 4. The distribution of the several species as a function of time is also seen in Figure 4.

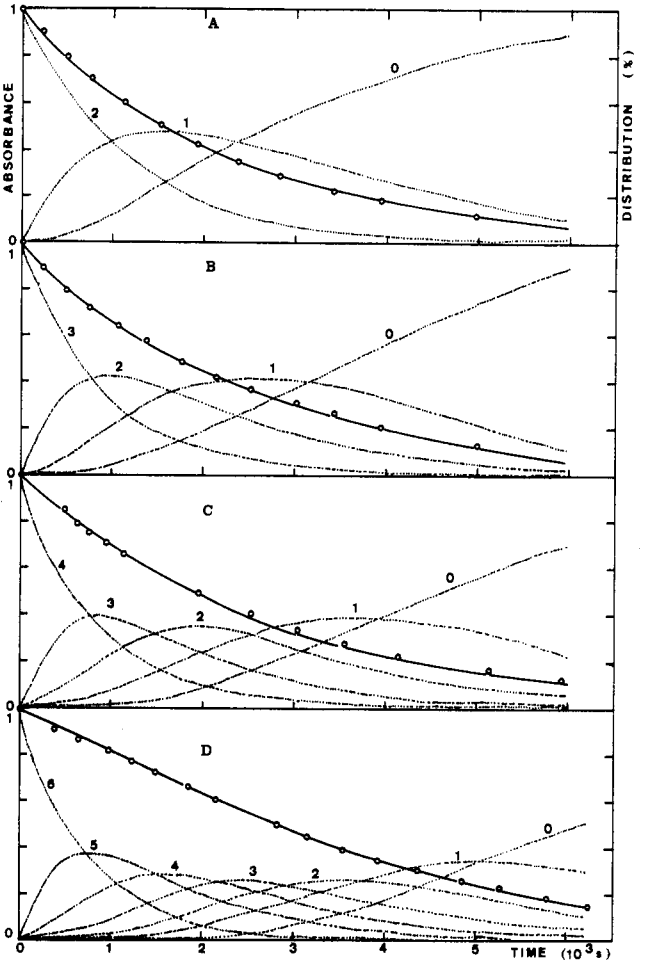

Figure 4. Normalized kinetic plots (circles) and theoretical fitting (solid lines) based on computational analysis (see text), for the dissociation reactions of the (A) trinuclear, (B) tetranuclear, (C) pentanuclear, and (D) heptanuclear $[Ru(bpz)_3(Fe(CN)_5)_n]^{(2-3n)+}$ complexes in aqueous solution, in the presence of 0.5 M Me_2SO, (ionic strength 0.100 M, 25 °C, pH 4.5). The dotted lines refer to the distribution plots of the several species containing n cyanoiron groups.

(20) Wherland, S.; Gray, H. B. *Proc. Natl. Acad. Sci. U.S.A.* **1976**, *73*, 2950.
(21) Toma, H. E.; Oliveira, L. A. A.; Giesbrecht, E. *Inorg. Chim. Acta* **1977**, *22*, 269.
(22) Capellos, C.; Bielski, B. H. J. "Kinetic Systems"; Wiley-Interscience: New York, 1972; p 46.

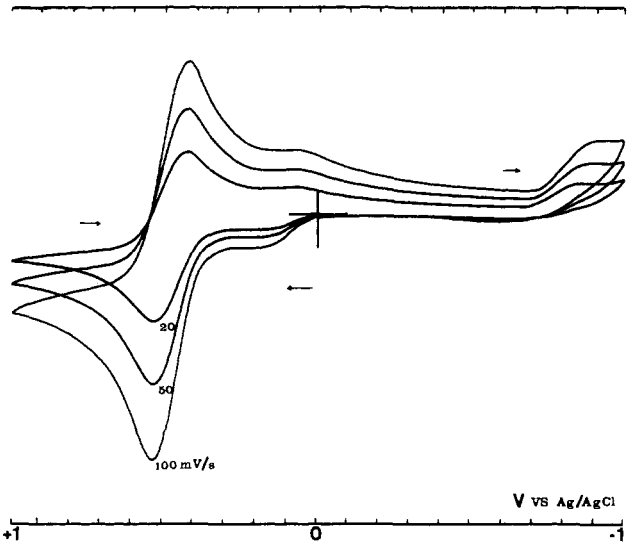

Figure 5. Cyclic voltammograms of the polynuclear $[Ru(bpz)_3(Fe(CN)_5)_6]^{16-}$ complex (8 mM, 0.3 M KCl, 0.20 M acetate buffer, 25 °C), in the presence of 2 mM excess of the pentacyanoferrate(II) ion, responsible for the shoulders at 0.1 V (add 0.222 V to convert to the NHE scale).

A similar procedure was employed for the dissociation kinetics of the 1:3 and 1:4 complexes, yielding k_{32} and k_{43} values of 1.10×10^{-3} and 1.2×10^{-3} s^{-1}, respectively. The consistency of the theoretical treatment can be seen in Figure 4B,C. From the kinetics of dissociation of the 1:6 complex, k_{65} and k_{54} were computed to be 1.30×10^{-3} and 1.25×10^{-3} s^{-1}, respectively, with use of the previously determined k_{ji} and ϵ_{ji} parameters, as illustrated in Figure 4D.

From the data shown in Table I, we can see that the relative stability of the several species is determined by the specific rates of substitution in the aquapentacyanoferrate(II) ion, which are sensitive to the electrostatic charges of the attacking polynuclear ligands. The kinetic constants for the dissociation reactions are around 4×10^{-4} s^{-1}, after correcting for the statistical factor, being similar to those previously reported for systems **3** and **4**. These data lead one to conclude that each $[Fe(CN)_5]^{3-}$ group binds essentially independently of any other.

Indeed given that the data adhere to eq 7 and that the dissociation rate constants are essentially independent of the number of bound pentacyanoferrate(II) groups, the results are consistent with the view that all the Fe–N bonds have essentially the same energy after factoring out the electrostatic term.

Electrochemistry. Cyclic voltammetry of the $Ru(bpz)_3^{2+}$ ion has been investigated previously in acetonitrile solutions containing tetraethylammonium hexafluorophosphate.[3] The half-wave potential for the Ru(III/II) couple is 2.08 V vs. NHE. The reduction waves for the bipyrazyl complex are observed at −0.56, −0.74, and −1.00 V.

The polynuclear ruthenium–iron complexes are insoluble in acetonitrile and in solvents like dimethylformamide, sulfolane, and dimethyl sulfoxide. For this reason, the electrochemistry was limited within the −1 to +1 V range, in aqueous solution.

The 1:1 dinuclear complex adsorbs on the glassy-carbon electrode, producing characteristic sharp peaks around 0.6 V. The cyclic voltammograms of the 1:2 to 1:6 complexes consist of a single pair of anodic/cathodic peaks, having reversible characteristics, with $E_{1/2} = 0.70$ V vs. NHE, as shown in Figure 5. The ratio between the anodic and cathodic peak currents was close to unity. The difference in potential between the anodic and cathodic peaks increases gradually from 60 to 90 mV, for the 1:2 to 1:6 complexes, respectively, with a nonlinear increase in the peak currents. These waves were ascribed to the monoelectronic Fe(II)/Fe(III) redox process associated with the $Fe(CN)_5(bpz)$ moieties. An additional irreversible cathodic wave was observed at −0.6 V (Figure 5), corresponding to the reduction of the $Ru(bpz)_3^{2+}$ center.

Electronic Spectra. The characteristic features of the electronic spectra may be summarized as follows:

A band is observed at 700 nm whose energy is almost independent of the number of bound $[Fe(CN)_5]^{3-}$ units. Note however that the absorption for the 1:1 complex is centered at about 690 nm.

A weak band is seen near 500 nm whose intensity grows with increasing number of $[Fe(CN)_5]^{3-}$ groups.

The band near 445 nm attributed to the Ru(d) → bpz($\pi^*(1)$) transition does not shift with increasing number of bound $[Fe(CN)_5]^{3-}$ groups but does appear to intensify slightly and become broader.

The shoulder near 340 nm is also independent of the $[Fe(CN)_5]^{3-}$ binding and is attributed to Ru(d) → bpz($\pi^*(2)$).[3,4]

The peak at 293 nm attributed to $\pi \rightarrow \pi^*$ (bpz) moves to 307.5 nm in the polynuclear species, a red shift of some 1600 cm^{-1}, rather less than that, 2650 cm^{-1}, observed in the protonated species.[4]

The existence of the band near 700 nm, attributed to Fe(II) → bpz(π^*), parallels those seen, for example, in $[Fe(CN)_5(pzMe^+)]^{2-}$ ($pzMe^+$ = methylpyrazinium) at 655 nm[8,23] and $[(bpz)(CN)_5Fe]^{3-}$ at 517 nm[24] and is additional proof of the binding between the Fe(II) atom and the peripheral nitrogen atoms of $[Ru(bpz)_3]^{2+}$.

Although we have no measurement for the Ru(III)/Ru(II) oxidation potential in the polynuclear species, it is reasonable that, at least for the mono-$[Fe(CN)_5]$ species, it is close to 2.0 V vs. NHE as in the unbound complex. The Fe(III)/Fe(II) redox potential is observed near 0.7 V, i.e. 1.3 V to lower energy. The energy separation between the 445- and 700-nm absorptions is 8200 cm^{-1}, slightly over 1.0 V. It is most probable therefore[24] that the acceptor orbital is the same for both transitions, with the 700-nm absorption assigned to Fe(d) → bpz($\pi^*(1)$).

The weak feature at 500 nm cannot be attributed to Ru(d) → bpz–$Fe(CN)_5(\pi^*)$ since such a charge-transfer transition would grow, with increasing number of pentacyanoferrate groups, at the expense of the intensity of the 445-nm Ru → bpz CT transition, which is definitely not the case. On the basis of the Ru CT spectra, the separation between bpz($\pi^*(1)$) and bpz($\pi^*(2)$) is about 7000 cm^{-1}. Adding this quantity to the energy of the Fe(d) → bpz($\pi^*(1)$) band at 700 nm would predict Fe(d) → bpz($\pi^*(2)$) to occur near 470 nm. This is close enough to 500 nm to suggest such an assignment for this feature. Thus the spectrum is assigned. No d → d transitions were identified.

One is led to conclude that the Ru(d) → bpz–$(Fe(CN)_5)_x$-($\pi^*(1)$) ($x = 0, 1, 2$) CT transitions all occur at essentially the same energy. Evidently binding of one or two $[Fe(CN)_5]^{3-}$ groups to each bipyrazine ring causes no shift in the Ru(d) → bpz(π^*) absorption, red shifts the bipyrazine $\pi \rightarrow \pi^*$ absorption slightly, and causes the Fe(d) → bpz(π^*) absorption, whose energy is independent of the number of $[Fe(CN)_5]^{3-}$ groups.

Associating these results with the kinetic and electrochemical data presented above confirms the view that, with the possible exception of the first $[Fe(CN)_5]^{3-}$ unit, each successive such unit binds independently of every other. The 1:1 complex differs in that the Fe → bpz(π^*) transition is shifted slightly to higher energy, and the first binding constant is slightly enhanced probably due to attraction between the positively and negatively charged reactants.

The absence of any shift in the Ru → π^* transition yet the presence of a shift in the $\pi \rightarrow \pi^*$ transition must require essentially no change in either the Ru(d) level or the bpz(π^*) levels yet a small destabilization of the π(HOMO) bipyrazine level, upon coordination by $[Fe(CN)_5]^{3-}$.

Reference to the literature reveals that the above data are rather unusual. The remote metal center should facilitate the Ru → bpz CT transition and shift the Ru(III)/Ru(II) redox potential gen-

(23) Lever, A. B. P. "Inorganic Electronic Spectroscopy", 2nd ed.; Elsevier: Amsterdam, The Netherlands, 1984.
(24) Toma, H. E.; Coelho, A. L.; Lever, A. B. P., research in progress. Note that the species $[(bpz)(CN)_5Fe]^{3-}$ appears to protonate initially at the cyanide rather than the bpz group.
(25) Dodsworth, E. S.; Lever, A. B. P. *Chem. Phys. Lett.* **1985**, *119*, 61.

erally more positive than the parent species.[26] Indeed binding of the $[Fe(CN)_5]^{3-}$ group to pyrazine (pz) in either $[Ru(NH_3)_5(pz)]^{2+}$ [9,26] or *trans*-$[Ru(NH_3)_4(pz)_2]^{14}$ results in a substantial red shift of the Ru → pz CT band (1940 and 2600 cm^{-1}, respectively).

It is suggested that the strong π-accepting ability of the cyanide groups induces the $[Fe(CN)_5]^{3-}$ group to behave as a σ Lewis acid, leaving the Ru(II) atom to bind the pyrazine in a π sense.[9] However, the appearance of the Fe → bpz(π^*) transition energetically below that seen in the methylpyrazinium $[(pzMe^+)(CN)_5Fe]^{2-}$ and $[(bpz)(CN)_5Fe]^{3-}$ species indicates that the $[Ru(bpz)_3]^{2+}$ group acts as an excellent π-acceptor especially as the E[Fe(III)/Fe(II)] potential is not significantly different from that observed previously in $[Fe(CN)_5L]^{3-}$ complexes.[9,26] The pK_a value for monoprotonation is −2.2,[4] and this value is probably appropriate for binding of all the pentacyanoferrate(II) groups. Thus the peripheral nitrogen atoms are very weak bases. In this case back-bonding from Fe(II) to bipyrazine probably plays a significant role, but the synergistic effects associated with the σ-bonding must conspire to cause no change in energy of either the bpz(π^*) or Ru(d) level.

The presence of two charge-transfer transitions allows one to extract further information where electrochemical data are also available.[25] Thus one may write[25,27]

$$E_{op}(Ru \rightarrow bpz(\pi^*)) = E[Ru(III)/Ru(II)] - E[Ru^{III}(bpz)Fe^{II}/Ru^{III}(bpz^-)Fe^{II}] + \chi_i(Ru \rightarrow bpz) + \chi_o(Ru \rightarrow bpz) \quad (12)$$

where the first potential is the Ru(III)/Ru(II) redox potential for this species bound to $([Fe^{II}(CN)_5]^{3-})_n$ and the second corresponds with reduction of bipyrazine bound to Ru(III) (and Fe(II)) and is not available by direct electrochemical experiment. The last two terms are the inner and outer reorganization energies for this transition.[23,25,28] Further we may write

$$E_{op}(Fe \rightarrow bpz(\pi^*)) = E[Fe(III)/Fe(II)] - E[Ru^{II}(bpz)Fe^{III}/Ru^{II}(bpz^-)Fe^{III}] + \chi_i(Fe \rightarrow bpz) + \chi_o(Fe \rightarrow bpz) \quad (13)$$

where the first potential is the observed Fe(III)/Fe(II) redox potential for this species and the second corresponds with reduction of bipyrazine bound to Ru(II) and Fe(III) and is not available by direct electrochemical experiment.

Suppose we assume that the reorganization energies for these two transitions are essentially identical. We may then write, for the differences in energy between the two transitions, the statement

$$E_{op}(Ru \rightarrow bpz(\pi^*)) - E_{op}(Fe \rightarrow bpz(\pi^*)) = 8200\ cm^{-1}$$

$$= E[Ru(III)/Ru(II)] - E[Ru^{III}(bpz)Fe^{II}/Ru^{III}(bpz^-)Fe^{II}] - E[Fe^{III}/Fe^{II}] + E[Ru^{II}(bpz)Fe^{III}/Ru^{II}(bpz^-)Fe^{III}] \quad (14)$$

The value of E[Ru(III)/Ru(II)] is 2.10 V (vs. NHE) for the parent species[3,29] and, given that the Ru(d) level is unaffected by coordination of the $[Fe(CN)_5]^{3-}$ groups, will also be the appropriate value for the heteropolynuclear species. The Fe(III)/Fe(II) reduction potential is measured to be +0.70 V, leading to the conclusion (1 eV = 8065 cm^{-1})

$$E_{op}(Ru \rightarrow bpz(\pi^*)) - E_{op}(Fe \rightarrow bpz(\pi^*)) = 8200\ cm^{-1}$$

$$1.02 = 2.10 - 0.70 - E[Ru^{III}(bpz)Fe^{II}/Ru^{III}(bpz^-)Fe^{II}] + E[Ru^{II}(bpz)Fe^{III}/Ru^{II}(bpz^-)Fe^{III}]$$

and hence

$$E[Ru^{II}(bpz)Fe^{III}/Ru^{II}(bpz^-)Fe^{III}] - E[Ru^{III}(bpz)Fe^{II}/Ru^{III}(bpz^-)Fe^{II}] = -0.38\ V \quad (15)$$

providing information about energy differences between mixed-valence isomers and being the energy for the electron-transfer process

$$Ru^{II}(bpz)Fe^{III} + Ru^{III}(bpz^-)Fe^{II} \rightarrow Ru^{III}(bpz)Fe^{II} + Ru^{II}(bpz^-)Fe^{III} \quad (16)$$

Acknowledgment. This work was supported by the CNPq and FINEP agencies in Brazil (H.E.T.). We appreciate discussion with Dr. E. S. Dodsworth.

Registry No. $[Ru(bpz)_3](PF_6)_2$, 80907-56-8; $Na_3[Fe(CN)_5NH_3]$, 14099-05-9; $Na[Ru(bpz)_3(Fe(CN)_5)]$, 99631-50-2; $[Fe(CN)_5(H_2O)]^{3-}$, 18497-51-3; $[Ru(bpz)_3(Fe(CN)_5)_2]^{4-}$, 99617-64-8; $[Ru(bpz)_3(Fe(CN)_5)_3]^{7-}$, 99631-51-3; $[Ru(bpz)_3(Fe(CN)_5)_4]^{10-}$, 99617-65-9; $[Ru(bpz)_3(Fe(CN)_5)_5]^{13-}$, 99617-66-0; $[Ru(bpz)_3(Fe(CN)_5)_6]^{16-}$, 99617-67-1.

(26) Moore, K. J.; Lee, L.; Mabbott, G. A.; Petersen, J. D. *Inorg. Chem.* **1983**, *22*, 1108.
(27) Lever, A. B. P.; Pickens, S. R.; Minor, P. C.; Licoccia, S.; Ramaswamy, B. S.; Magnell, K. *J. Am. Chem. Soc.* **1981**, *103*, 6800.
(28) Dodsworth, E. S.; Lever, A. B. P. *Chem. Phys. Lett.* **1984**, *112*, 567; **1985**, *116*, 254.
(29) Gonzales-Velasco, J.; Rubinstein, I.; Crutchley, R. J.; Lever, A. B. P.; Bard, A. J. *Inorg. Chem.* **1983**, *22*, 822.

Contribution from the Institut für anorganische Chemie, Universität Bern, CH-3000 Bern 9, Switzerland

Trends of Magnetic Interactions in Related Transition-Metal Dimers

B. Leuenberger and H. U. Güdel*

Received February 19, 1985

Exchange parameters determine the magnetic properties of transition-metal dimers. They can be related to MO energy differences obtained by extended Hückel calculations. Good agreement with experiment is obtained in the series $Cr_2X_9^{3-}$ (X = Cl, Br, I). The observed trends in the series $Ti_2Cl_9^{3-}$, $V_2Cl_9^{3-}$, $Cr_2Cl_9^{3-}$ are reproduced semiquantitatively by the model. The extended Hückel technique is not able to account for the observed large increase of the exchange coupling between $Cr_2Cl_9^{3-}$ and $V_2Cl_9^{5-}$. The experimental ratio of the orbital exchange parameters in $V_2Cl_9^{5-}$, $J_a/J_e = 36$, is exactly reproduced by the calculation. In $[(en)_2Cr(OH)_2Cr(en)_2]^{4+}$ the relative contributions to the total J of the various orbital parameters are reasonably accounted for by the model.

Introduction

Dimers of transition-metal ions are well suited to the study of the nature of magnetic interactions, i.e. exchange coupling. Many compounds have been studied in which the transition-metal ions occur as pairs either by nature or by doping a diamagnetic host lattice with a small amount of a transition metal.[1] In most cases the ground-state exchange parameter J was determined, and for

(1) Willett, R. D., Ed. "NATO ASI on Magneto-Structural Correlations in Exchange-Coupled Systems"; Reidel: Amsterdam, 1985.

0020-1669/86/1325-0181$01.50/0